Applied Energy 238 (2019) 1484–1496

Contents lists available at ScienceDirect

Applied Energy

journal homepage: www.elsevier.com/locate/apenergy

High-resolution multi-objective optimization of feedstock landscape design for hybrid first and second generation biorefineries

Trung H. Nguyen[a,b,*], Julien Granger[c], Deval Pandya[d], Keith Paustian[a,b]

[a] Department of Soil and Crop Sciences, Colorado State University, USA
[b] Natural Resource Ecology Laboratory, Colorado State University, USA
[c] Shell Trading (U.S.) Company, USA
[d] Shell Global Solutions (U.S.) Inc., USA

HIGHLIGHTS

- Combining crops and residues for large-scale hybrid biofuels production.
- Linking spatial models with optimization algorithms to assess sustainability.
- Modeling feedstock production at high spatial and temporal resolutions.
- Using 3D Pareto surfaces to identify unfavorable tradeoffs among design objectives.
- Discussing how changes in social costs of C and N affect optimal solutions.

ARTICLE INFO

Keywords:
Biofuel supply chain
Multi-objective optimization
Feedstock landscape design
Life cycle assessment
Ecosystem modeling
Ecosystem services

ABSTRACT

Biofuels have been proposed as a potential solution for climate change mitigation. However, there exist several barriers, such as "food vs fuel" issues and technological constraints, restricting the sustainable commercialization of both first- and second-generation biofuels. Combining arable crops and their residues for hybrid first- and second-generation biofuel production provides opportunities to overcome these barriers. This study presents a high-resolution quantitative tool to support decision-making in feedstock production and sourcing for hybrid biofuel supply chains. We demonstrate this work with a case study on optimizing feedstock landscape design for a hybrid corn grain- and stover-based ethanol production system at Front Range Energy biorefinery, Windsor, Colorado, USA using a coupled simulation modeling and life-cycle assessment approach. The case study considered three competing design objectives including the minimization of feedstock-delivered costs, farm-to-refinery greenhouse gas emissions (GHG), and nitrogen (N) leaching, subject to constraints in land use and biofuel feedstock demand. Social costs of carbon (SC-CO_2) and nitrogen leaching (SC-NL) were used as weighting factors for GHG and N leaching in the objective function. Our results showed that marginal decreases of feedstock-delivered costs (below \$0.31 L^{-1}), N leaching (below 0.44 g N L^{-1}), and GHG emissions (below 125 g CO_2e L^{-1}) resulted in extreme trade-offs among the design objectives. Changes in feedstock landscape design were most sensitive to the variations of the SC-CO_2 between \$400 and \$800 per Mg CO_2e, SC-NL between \$0 and \$50 per kg N leaching, and their ratio between 0 and 350, respectively.

1. Introduction

Biofuels have received considerable attention as part of a solution to reduce dependency on petroleum and reduce net CO_2 emissions from fuel use. In particular, the European Union has targeted a 10% share of energy from renewable sources, including biofuels, by 2020 in the transport sector while the United States Renewable Fuels Standard 2 mandated an annual production target of 136 billion liters of biofuels by 2022 [1]. Biofuels can be derived from many sources including food crops such as corn grain and sugarcane (first-generation) or ligno-cellulosic materials from crop and forest residues or dedicated grasses (second-generation). Compared to the second-generation, first-generation technology is more commercially mature. However, its sustainability is currently debated due to the potential threats on food supplies

* Corresponding author at: Department of Soil and Crop Sciences, Colorado State University, 307 University Ave., Bldg.: Plant Sciences C127, Fort Collins, CO 80523-1170, USA.
E-mail address: nguyentrung1710@gmail.com (T.H. Nguyen).

https://doi.org/10.1016/j.apenergy.2019.01.117
Received 10 August 2018; Received in revised form 11 October 2018; Accepted 17 January 2019
Available online 31 January 2019
0306-2619/

and biodiversity and consequential impacts of indirect land use change on total greenhouse gas (GHG) emissions [2–5]. Second-generation biofuels have been proposed to address these problems since they can use non-food sources as feedstock and marginal land for feedstock production. Nevertheless, due to the immature market structure and conversion technology, commercially viable production of second-generation biofuels is still challenging [6].

Combining arable crops and their residues such as corn grain and corn stover for a hybrid first-and second-generation biofuels production provides a potential solution to the large-scale and sustainable production and use of biofuels. This solution takes advantage of first-generation infrastructure but requires less productive land to secure the biomass feedstock, thus imposing less pressure on food commodities and biodiversity. However, this coupling necessitates further efforts to design and develop more sustainable and robust biofuel supply chains, emphasizing multiple feedstocks production and management.

Although there has been a relatively large number of works on analyzing and optimizing biomass energy supply chains, Yue et al. [7] pointed out that most of the studies focused on the sole production of first-generation (e.g., [8–10]) or second-generation biofuels (e.g., [11–13]). To date, there has been limited research attempting to optimize biomass supply chain for hybrid first- and second-generation biofuel systems [14–17]. In addition, optimization problems have been mainly directed towards supply chain logistics, especially the design of transportation networks and facility siting, using mathematical-programming-based tools such as Mixed Integer Programming. These studies also optimized based on the tactical levels at coarse spatial resolutions such as five-square-mile hexagons [18], hydrological response units (HRU) (> 204 ha) [19], and watershed [20] scales. There are presently few studies that focus on optimizing feedstock cultivation and land management in a spatially-explicit manner with high spatial and temporal resolutions [21–24]. We believe that this is important to harness the "management swing potential" [25] between different biofuel feedstocks, especially in hybrid and multiple-feedstock biofuel systems, to obtain the most cost-effective and sustainable biofuel production.

The formulation of optimization problems using mathematical-programming approaches in previous studies has advantages in terms of model generalization, simulation efficiency, and exact solution search. These approaches also fit many supply chain logistic problems such as transportation or process design and operation at strategic and tactical levels. However, for higher-resolution optimization of biofuel feedstocks cultivation and land management, these approaches are poorly-suited since it is inadequate to use a set of simplified equations to depict the dynamic ecosystem changes induced by different land management. Such changes are the results of complex and non-linear interactions among site-specific weather conditions, soil properties, crop types, cropping practices and land use history [26]. For example, high biomass removal rates increases feedstock yield but also affects subsequent farming input requirements, CO_2 emissions from soil carbon stock change, susceptibility to erosion and other ecosystem services [25]. The extent of these subsequent impacts depends on topography, feedstock types, weather and soil conditions, and many other factors. Accurately capturing these changes in the optimization is the key to finding true optimum solutions for biofuel supply chain design.

The use of biophysical models offers more detailed quantification of cropping system changes associated with the changes in land management [27,28]. These models such as CENTURY [29], DayCent [30], DNDC [31], RothC [32], and APSIM [33] can better represent site-specific interactions of biophysical characteristics (e.g., climate and soil characteristics). They can also capture the current and historical influence of land use and management practices on potential future changes in many ecosystem functions such as soil carbon stocks [34]. The coupling of biophysical models with geographic information system (GIS) and optimization algorithms such as the Agricultural Ecosystem Service Optimization" (Ag-EcoSOpt) system [22] provides useful platforms for the spatially-explicit quantification and optimization of agricultural ecosystem service provisioning, as well as estimates of feedstock production for biofuel supply chains at very high spatial resolutions (field and sub-field scales). The Ag-EcoSOpt uses a process-based biogeochemical model (DayCent) for exploratory landscape simulations to investigate the production potential of a cropping system. The simulated outcomes can then be optimized with mathematical algorithms for different design and management objectives. The resulting solutions can be shown and analyzed via maps and graphs to support decision-making. Although, this approach is a discrete optimization, fine-scale exploratory simulations of the target systems (i.e., better inputs for optimization) will likely result in approximate solutions that are very close to the global optimum for any biofuel supply chain optimization problems.

Multi-objective optimization has also been used in many studies to optimize for competing objectives within biofuel supply chain design and management (e.g., [35,21,9,13,36,20,37,19]). This type of optimization typically generates a set of Pareto-optimal solutions (also called non-dominated solutions) where any improvement in one objective always impairs some others. The goal of multi-objective optimization is to help the decision maker find a solution that is preferable to them. We found that a majority of previous studies have focused on bi-objective optimizations of costs and greenhouse gas emissions or water footprints for biofuel supply chain. Only a few studies considered more than two design objectives [38,20,39,19]. When it comes to ecosystem-level impact analysis, Čuček et al. [40] argued the importance of considering other environmental criteria in the supply chain optimization such as nitrogen, land use, and biodiversity footprints. Despite the large body of research on optimizing biofuel supply chains, to the best of our knowledge, there have been no studies that have demonstrated multi-objective optimization of multiple feedstock cultivation for hybrid biofuel supply chains at high spatial and temporal resolutions.

This study aims at demonstrating a robust approach that facilitates the spatially-explicit and multi-objective optimization of hybrid biofuel supply chains, focusing on the design of feedstock landscapes and the identification of optimum land management. We present this work with a case study on a tri-objective optimization of feedstock landscape design for a hybrid first- and second-generation ethanol production at Front Range Energy biorefinery (FRE), Windsor, Colorado, USA. The case study considered three competing objectives including the minimization of feedstock-delivered costs, farm-to-refinery greenhouse gas emissions, and nitrogen leaching at a high spatial resolution (field scale) with detailed consideration of historical land use (dating back to the 1880s).

2. Method

2.1. Study site

The Front Range Energy (FRE) biorefinery is a local fuel ethanol supplier with a capacity of 1.51×10^8 L of ethanol per year (~ 40 million U.S. gallons per year). Our analysis assumed that FRE can produce both first generation and cellulosic biofuels and that the feedstock comes mainly from corn grain and corn stover in the study region. Corn stover is the residue of stalk, leaf, husk, and cob left behind following a corn harvest. The targeted feedstock production area is comprised of 55,401 ha of irrigated corn fields in six counties within an 80 km-radius (~ 50 miles) surrounding the biorefinery, including Adams, Boulder, Broomfield, Larimer, Morgan, and Weld counties (Fig. 1). These counties are located in north-central Colorado, and are among the most productive irrigated agricultural regions in the state with a majority of fine-loamy soils, an average annual rainfall of 38 cm, an average July high temperature of 30.6 °C, and an average January low temperature of -8.5 °C [41].

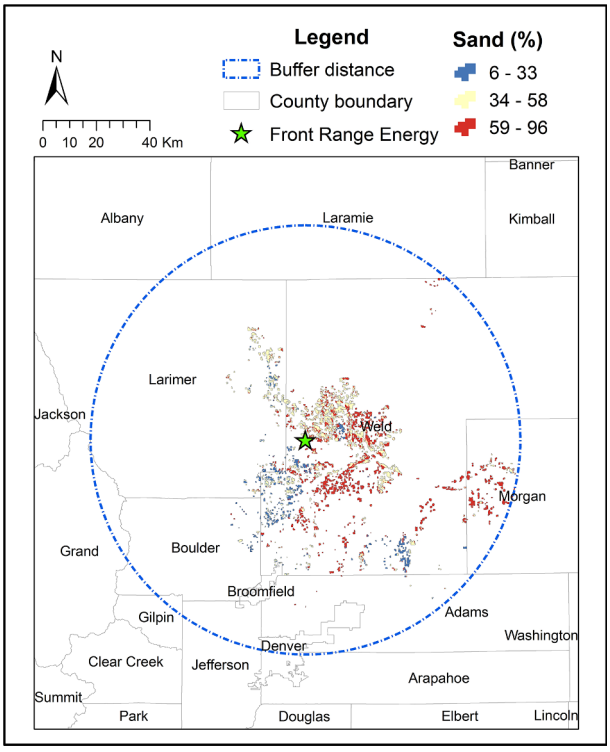

Fig. 1. Irrigated corn land units with the percent sand content of the soils within the study region. The blue circle is the 80 km-radius buffer around Front Range Energy. (For interpretation of the references to colour in this figure legend, the reader is referred to the web version of this article.)

2.2. Scope of the analysis

The main objective of this case study was to identify the Pareto surface for the trade-offs among three competing design objectives including minimization of feedstock-delivered costs, farm-to-refinery greenhouse gas emissions (GHG), and nitrogen (N) leaching. For each Pareto-optimal solution on the surface, we also identified the spatial configuration of the feedstock landscape as well as the optimum management practices (e.g., rates of N fertilization, irrigation, stover removal, and tillage intensity) for each corn field in the landscape. The corresponding ratio between grain-based and stover-based ethanol was also calculated.

Our study used the life cycle optimization framework outlined in Yue et al., [37]. This framework follows the first three phases (goal and scope definition, inventory analysis, and impact assessment) of a classical life cycle assessment (LCA) [42], and performs the last phase (LCA interpretation) by coupling optimization tools with impact assessment. The system boundary for our optimization analysis was from field to biorefinery gate. The functional unit used to compare the GHG intensity of ethanol and conventional gasoline (CG) was one megajoule (MJ). Farm-to-refinery emissions for grain- and stover-derived ethanol were calculated using detailed, high-resolution data in our analysis and then extended using refinery-to-wheel emissions reported in the literature to estimate the full attributional GHG reductions of biofuels relative to CG. The reference life-cycle emission of CG used in our study was 94 g MJ^{-1} [43].

Since corn grain and corn stover were treated as two feedstocks for biofuel production in our analysis, we applied the process-level co-product handling method to allocate cost and environmental burdens between the two products [44]. This method assigns the burdens of individual process steps within the system boundary to the product that is responsible for the existence of those steps. The burdens of the shared steps and components can be allocated between co-products based on their energy contents or market values. In this analysis, market values were used to allocate the costs and environmental burdens between co-products. We used a 10-year averaged U.S. corn grain price of \$180 Mg^{-1} reported by Ycharts (https://ycharts.com/) for the period from 2007 to 2017 and an average stover price of \$70 Mg^{-1} reported by Thompson and Tyner [45].

The Agricultural Ecosystem Service Optimization (Ag-EcoSOpt) tool [22] was employed to simulate changes in ecosystem indicators at a high spatial resolution under variations in management practices. The Greenhouse Gases, Regulated Emissions, and Energy Use in Transportation Model – commonly known as GREET [46] – was used to calculate fossil fuel-derived emissions associated with farm operations and feedstock transportation. The supply chain financial budgeting was carried out using empirical data. The optimization problem was formulated in PuLP [47], a Python-based linear programing (LP) model, and solved by CPLEX solver [48]. We used the weighted sum method to iteratively solve the multi-objective optimization problem and employed the natural neighbor interpolation method to approximate the Pareto surface representing trade-offs among the three design objectives.

2.3. Landscape modeling of the study site

2.3.1. Agricultural ecosystem service optimization tool

The Ag-EcoSOpt tool includes a core biogeochemical model (DayCent), a database of historical land use for U.S. cropland, a geospatial component for spatially-explicit processing of inputs and outputs from DayCent's landscape simulations, and an optimization component for land use and land management decision making. The DayCent model [49,30] is a daily time step process-based model that simulates the dynamics of biogeochemical flows of carbon and nitrogen among the atmosphere, vegetation, and soil. The model has been widely used to study soil carbon and nitrogen dynamics, and soil greenhouse gas (CO_2, N_2O, CH_4) emissions especially for agricultural ecosystems [50–56,23].

The site-specific input data needed to initialize and run DayCent include weather (i.e. daily maximum and minimum air temperature, daily precipitation), soil properties, vegetation types, land use history, and management practices (e.g., irrigation, tillage, fertilization). These input data were acquired for the study region through the Ag-EcoSOpt's automated geospatial component from several spatial databases (Table 1). The shapefiles of these databases were then intersected to create 4782 polygons of various sizes representing irrigated corn fields in the study site, including 673 unique combinations of soil and weather data (DayCent input strata) (Fig. 1). Each unique stratum was simulated with DayCent and the results were linked back to their associated landscape polygons for optimization and spatial visualization.

For each input stratum, DayCent was initialized using historical land use information from the Ag-EcoSOpt database. The database contains pre-settlement and historical agricultural land use assumptions for Major Land Resource Areas (MLRA) up to 1979 [57]. The stratum was then extended with the simulation of a business-as-usual scenario (BAU) for corn production from 1980 to 2016. The BAU scenario for Colorado's irrigated corn crop was 170 kg of nitrogen per hectare, 34 cm of irrigated water per growing season, 75% residue removal, and conventional tillage [58]. The exploratory landscape simulation was

Table 1
Summary of spatial data inputs.

Spatial database	Data type	Year	Native Resolution	Source
SSURGO	Soils	2014	1:12,000–1:63,360	[95]
NARR	Daily weather	1979–2010	32 km	[41]
MIrAD-US	Irrigation extent	2007	250 m	[96]
Crop Data Layer	Crop types	2016	30 m	[97]

continued from the BAU for a 30-year period (from 2017 to 2047) under the management practice scenarios defined in Section 2.3.2. These simulations were executed in parallel on an 18-node, 216-processor cluster computing system at Colorado State University's Natural Resources Ecology Laboratory. The detailed modeling process was described by Nguyen et al., [22] where the authors used Ag-EcoSOpt to simulate corn production in South Platte River Basin, Colorado, USA.

2.3.2. Scenarios for exploratory landscape simulations

Besides the BAU scenario, we performed a combinatorial set of simulations for every corn field in the landscape, for a total of 180 management scenarios permuting five N fertilization rates, four irrigation rates, three stover removal rates, and three levels of tillage intensity. Five N fertilization rates, comprising 70, 110, 150, 190, and 230 kg N ha^{-1}, were chosen to reflect a common range of fertilization for irrigated continuous corn in the area [59]. Irrigation rates were dynamically calculated from soil-specific field capacity (FC). We simulated four levels of irrigation representing full irrigation to 100% FC, and three limited irrigations at 80%, 60%, and 40% FC. Our limited irrigation scenarios were characterized by the reduction in the amount of irrigated water applied. The three rates of stover removal were 22, 52, and 83% of the total residue. These rates represented low, moderate and high stover harvest scenarios, respectively [60]. We also simulated three levels of tillage intensity, including conventional tillage (CT), reduced tillage (RT), and no-till (NT). Conventional tillage was defined as multiple tillage operations every year with significant soil inversion through moldboard plowing. Reduced tillage lessened soil inversion by using chisel plowing. No-till was defined as not disturbing the soil except through the use of fertilizer and seed drills [57]. The outputs from the combinatorial simulation of 181 management scenarios on 4782 corn fields in the landscape were used in the optimization.

2.4. Calculation of objective metrics at the farm level

2.4.1. Feedstock-delivered costs

The feedstock-delivered costs for a particular farm included the farm production costs and the costs to transport the produced feedstocks to the refinery gate. The economic data used for calculating feedstock-delivered costs were obtained from different sources [45,61–63], as reported in Supplemental Materials S1. All the monetary values acquired from the literature were adjusted for inflation to 2017 US dollars. Farm production costs included tillage-based fixed costs and variable costs of N fertilization and irrigation, land rent, and feedstock-dependent costs for harvest, grain drying, storage, and handling. Feedstock transport costs were calculated based on feedstock yields and the transport distance from each field to the FRE refinery. The Euclidean distances from fields to the biorefinery were calculated through Ag-EcoSOpt's geospatial component. DayCent reports corn grain and harvested stover as grams of carbon per square meter. We converted corn grain and harvested stover to Mg of dry matter (d.m) per hectare per year (averaged over entire simulation period) assuming 43.5% carbon content and moisture content of 15.5% for corn grain and 20% for harvested stover [64]. All commodity prices were treated as exogenous and static regardless of management practice changes in the analysis.

2.4.2. Farm-to-refinery greenhouse gas emissions

The farm-to-refinery GHG emissions associating with biofuel feedstock production included soil, farm operation, and feedstock transport emissions. Soil emissions were calculated based on soil-related emission sources modeled with DayCent, including annual CO_2, N_2O, and CH_4 emissions [65]. The annual net soil CO_2 emission from soil heterotrophic respiration was calculated by taking the difference between SOC levels of every two consecutive years. Annual N_2O emission consisted of direct and indirect N_2O emissions. The direct N_2O emission was reported by DayCent in term of N_2O efflux, while the indirect N_2O emissions were computed from volatilized N (NO_x + NH_3) fluxes and nitrogen leaching with the emission factors (EF) of 0.01 and 0.075, respectively [65]. Annual N_2O and CH_4 were converted into carbon dioxide equivalent (CO_2e) by using their 100-year global warming potential values (GWP_{100}) [66].

To calculate GHG emissions associated with farm operations and feedstock transportation, we used the Greenhouse Gases, Regulated Emissions, and Energy Use in Transportation Model (GREET) [46]. The GREET's default pathway for Integrated Corn/Stover Ethanol was updated with our specific inventory data. GREET's soil emissions were replaced with site-and-management specific values modeled with DayCent. Since we only focused on the effects of N fertilizer use, we assumed the same P application rate of 76.21 kg P ha^{-1} for all scenarios. No K fertilizer, manure, or lime applications were simulated in our analysis. The amounts of herbicide (7 g per Mg of d.m corn grain) and insecticide (0.06 g per Mg of d.m corn grain) were taken from the GREET's default repository for corn farming and were assumed as application rates for conventional tillage. The herbicide and insecticide application rates were increased by 4% for reduced tillage, and 47% for no-till compared to those of conventional tillage, as reported in Penn State Extension [67]. We did not consider the GHG emissions associated with the production and manufacture of the fertilizers and farm equipment.

The information on fuels used for farm operation were obtained from different sources [68,69,61] to compute the average energy use for different tillage types in our analysis (Supplemental Materials S2). The energy use for irrigation was 107,242 Btu cm^{-1}, calculated based on the method presented in Martin et al., [70] assuming an average pumping lift of 80-feet and a pump discharge pressure of 45 lb per square inch.

Corn grain was assumed to be transported to the stack by medium-heavy duty truck (MHDT) and from the stack to the refinery by heavy-heavy duty truck (HHDT). Corn stover was assumed to be transported by MHDT from field to the refinery in the form of dry bales. The transportation emissions were calculated with GREET's default emission factors and the Euclidean distances from farms to the refinery. The emission factors used in our analysis are summarized in Table 2. The farm-to-refinery GHG emissions for each farm were reported in terms of Mg of CO_2e per hectare per year.

2.4.3. Nitrogen leaching

Nitrogen (N) leaching due to corn grain and stover production for ethanol was calculated by the nitrogen submodel in DayCent. DayCent calculates N leaching in each farm as a function of soil nitrate (inorganic N leaching) and active soil SOM pool decomposition (organic N leaching), soil texture, and the amount of water moving through the soil profile N leaching was reported in the unit of gram of N per square meter by DayCent and was converted to kg of N per hectare per year averaged over the entire simulation period.

Table 2
GREET's emission factors for farm operation and feedstock transport.

Emission source	Unit	Emission factor
Farm energy	g CO_2e MJ^{-1}	90
N fertilizer	g CO_2e g^{-1}	3.9
P fertilizer	g CO_2e g^{-1}	1.5
Herbicide	g CO_2e g^{-1}	20
Insecticide	g CO_2e g^{-1}	23
Storage and handling of stover	g CO_2e Mg^{-1}	1167
Corn transportation	g CO_2e Mg^{-1} km^{-1}	208
Stover transportation	g CO_2e Mg^{-1} km^{-1}	240
Corn ethanol refinery-to-wheel emissions	g CO_2e MJ^{-1}	35
Stover ethanol refinery-to-wheel emissions	g CO_2e MJ^{-1}	16

2.5. Multi-objective optimization of feedstock landscape design

2.5.1. Formulation of the optimization problem

To integrate different competing design objectives for linear programming, we used the weighted sum method (WS) [71]. This method converts a multi-objective optimization problem into a single-objective one using a substitute objective function. Each objective was assigned a weight relative to its importance in decision-making and the weighted sum of all objectives was then be optimized. Since WS method is only applicable when all objectives are expressed in the same unit, we monetized GHG emissions and N leaching by multiplying their actual values with the corresponding social costs, where the social costs of GHG emissions (SC-CO_2) and N leaching (SC-NL) were defined as the estimated damages to the ecosystem in monetary term caused by an incremental increase in CO_2e emissions and N leaching, respectively [72,73]. These metrics are normally calculated using integrated assessment models that translate GHG emissions or N leaching into potential ecosystem impacts and then calculating a monetary cost to those impacts in dollars per year [72]. They are subsequently used by government agencies to evaluate federal regulations. However, in our analysis, these metrics were used to weigh the importance of GHG emissions and N leaching in the multi-objective optimization. As a result, they were allowed to vary from 0 (excluding a certain objective) to infinity (single objective optimization). The multi-objective optimization problem was formulated as follows, with detailed nomenclature presented in Table 3:

Let $i \in \{1, \dots, NF\}$ be the corn fields in the landscape and $j \in \{1, \dots, MP\}$ be the management practice scenarios of each corn field. (NF = 4782, MP = 181).

For all i, let $x_{i,j} \in \{0, \dots, 1\}$ be the fraction of field i where management practice scenario j is chosen. We assumed that a field can be divided into subfields for multiple management practice scenarios.

Objective:

$$\text{Min} \sum_i^{NF} \sum_j^{MP} x_{i,j} * (w_1 * \text{Cost}_{i,j} + w_2 * (SC - CO_2 * GHG_{i,j}) + w_3 * (SC - NL * NL_{i,j})) \quad (1)$$

Subject to (s.t.):

$$x_{i,j} \in \{0, \cdots, 1\} \quad (2)$$

$$\sum_j^{MP} x_{i,j} \leq 1, \quad \forall\, i \in NF \quad (3)$$

$$TC = \sum_i^{NF} \sum_j^{MP} x_{i,j} * CY_{i,j} \quad (4)$$

$$TS = \sum_i^{NF} \sum_j^{MP} x_{i,j} * SY_{i,j} \quad (5)$$

$$EtOH = TC * CTE + TS * STE \quad (6)$$

$$EtOH \geqslant EtOHcap \quad (7)$$

$$Rg = \frac{\sum_i^{NF} \sum_j^{MP} x_{i,j} * GHGg_{i,j}}{TC * CTE * LHVe} \quad (8)$$

$$Rs = \frac{\sum_i^{NF} \sum_j^{MP} x_{i,j} * GHGs_{i,j}}{TS * STE * LHVe} \quad (9)$$

$$\frac{GS - (Rg + Wg)}{GS} * 100 \geq 20\% \quad (10)$$

$$\frac{GS - (Rs + Ws)}{GS} * 100 \geq 60\% \quad (11)$$

The objective (1) represents the minimization of feedstock-delivered costs, GHG emissions, and N leaching associated with the feedstock production for both grain- and stover-derived ethanol. The importance

Table 3
Nomenclature of the optimization problem.

Name	Description
Indices	
i	Index for fields in the landscape
j	Index for management practice scenarios in field i
Set sizes	
NF	Number of corn fields in the landscape (NF = 4782)
MP	Number of considered management practices for each field (MP = 181)
Parameters	
$Cost_{i,j}$	Feedstock-delivered costs of field i under management practice scenario j ($ year^{-1})
$GHG_{i,j}$	Farm-to-refinery GHG emissions of field i under management practice scenario j (Mg CO_2e year^{-1})
$NL_{i,j}$	N leaching of field i under management practice scenario j (kg N year^{-1})
SC-CO_2	Social cost of GHG emissions ($ per Mg CO_2e)
SC-NL	Social cost of N leaching ($ per kg N)
w_1	Weighting coefficient for feedstock-delivered costs
w_2	Weighting coefficient for GHG emissions, set to 1 for convenience (see Section 2.4.2)
w_3	Weighting coefficient for N leaching, set to 1 for convenience (see Section 2.4.2)
TC	Total corn grain used for grain-based ethanol production (Mg d.m year^{-1})
TS	Total harvested stover used for stover-based ethanol production (Mg d.m year^{-1})
EtOH	The total amount of ethanol produced from corn grain and harvested stover (L year^{-1})
CTE	Corn grain to ethanol ratio (CTE = 429 L Mg^{-1} (113.4 gallons Mg^{-1}))
STE	Stover to ethanol ratio (STE = 355 L Mg^{-1} (93.7 gallons Mg^{-1}))
EtOHcap	Ethanol production capacity of FRE (EtOHcap = 1.51 × 10^8 L year^{-1})
Rg	Farm-to-refinery GHG emissions of grain-based ethanol (g CO_2e MJ^{-1})
Rs	Farm-to-refinery GHG emissions of stover-based ethanol (g CO_2e MJ^{-1})
$GHGg_{i,j}$	Farm-to-refinery GHG emissions attributed to corn grain production for farm i under management practice scenario j (g CO_2e Mg^{-1})
$GHGs_{i,j}$	Farm-to-refinery GHG emissions attributed to stover production for farm i under management practice scenario j (g CO_2e Mg^{-1})
LHVe	Lower heating value of ethanol (LHVe = 21.2 MJ L^{-1})
Wg	Refinery-to-wheel GHG emissions of grain-based ethanol (Wg = 34 g CO_2e L^{-1})
Ws	Refinery-to-wheel GHG emissions of stover-based ethanol (Ws = 15 g CO_2e L^{-1})
GS	Well-to-wheel GHG emission of conventional gasoline (GS = 94 g CO_2e L^{-1})
Binary variables	
$x_{i,j}$	models the fraction of field i and the corresponding management practice scenario j is chosen in the final feedstock landscape for FRE.

of each design objective in the integrated objective function was expressed by their weighting coefficients. The constraints (2) and (3) allow the selection of multiple management scenarios for each corn field as long as the sum of their corresponding areal fractions does not exceed 1. The constraints (4), (5), (6), and (7) ensure that enough corn grain and stover are produced to meet the feedstock demand for 1.51×10^8 L of ethanol per year. We assumed that if a field is chosen as a feedstock site, all the corn grain and harvested stover from that field will be used for ethanol production. Corn grain and stover biomass were converted to ethanol using the conversion ratios of 429 L per Mg of d.m corn grain ($\sim$113.4 Gal Mg^{-1}) and 355 L per Mg of d.m corn stover ($\sim$93.7 Gal Mg^{-1}), respectively [46]. The constraints (8), (9), (10), and (11) require at least 20% and 60% reductions in life-cycle GHG emissions of grain-based and stover-based ethanol versus conventional gasoline, respectively. This is pursuant to the U.S. Environmental Protection Agency's (EPA) approved fuel pathways under the Renewable Fuel Standard 2 Program [1]. This set of constraints is driven by the co-product handling method and might produce different solutions depending on the allocation of GHG emission burdens between corn grain and corn stover.

2.5.2. Pareto surface simulation

Any adjustment in the weighting coefficients or social costs will likely result in changes in the integrated objective value (Eq. (1)), thus generating a different Pareto-optimal solution for the landscape design. Varying the weighting coefficients w_2 and w_3 might be appropriate when one wants to examine the trade-offs among the design objectives at a specific valuation of SC-CO_2 and SC-NL. However, for studies that aim to assess the effects of different SC-CO_2 and SC-NL on optimum landscape designs like ours, the variation of both weighting coefficients and social costs might add unnecessary complexities to the analysis. Therefore, we decided to fix the weighting coefficients w_2 and w_3 at 1 while varying SC-CO_2 and SC-NL to generate the Pareto-optimal set. The weighting coefficient w_1 was permitted values of 1 and 0 to allow the inclusion or exclusion of the feedstock-delivered costs objective in the optimization. The steps used to create the Pareto-optimal set are shown in Fig. 2. Each of the Pareto-optimal solutions can be defined by a set of three design objective values (i.e., the landscape summations of feedstock-delivered costs, GHG emissions, and N leaching), and thus lies on a Pareto surface, which is the 3-D graphical presentation of all

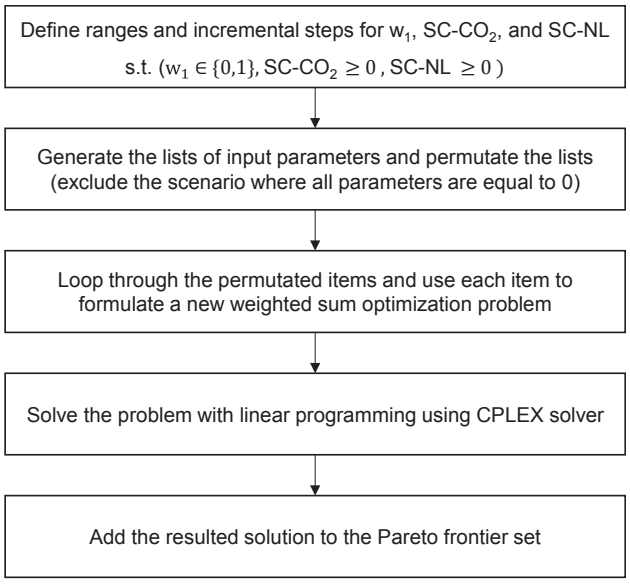

Fig. 2. Pareto frontier set simulation. The SC-CO_2 and SC-NL denote social costs of CO_2 and N leaching, and w_1 is the weighting factor for feedstock-delivered costs.

Table 4
Objective coefficients for corner objective scenarios.

Objective scenario	Parameters		
	w_1	SC-CO_2	SC-NL
Minimizing feedstock-delivered costs (minCost)	1	0	0
Minimizing farm-to-refinery emissions (minGHG)	0	1	0
Minimizing N leaching (minNL)	0	0	1

the Pareto-optimal solutions. The extent of the Pareto surface was identified by iteratively solving bi-objective optimization problems (ignoring one objective). When only one objective was minimized, the algorithm generated a corner solution representing the approximation of global minimum for that objective. We simulated the corner solutions for all design objectives based on the setup in Table 4. To compare the first- and second-generation ethanol with their hybrid, we also simulated the corner solutions for scenarios where either only corn grain or only corn stover was used as feedstock to produce 1.51×10^8 L year^{-1}.

Since it is impossible to identify all points on a surface, we used interpolation techniques to construct the Pareto surface based on the simulated Pareto-optimal set. The natural neighbor interpolation [74] was employed in this study through gridata function in MATLAB curve fitting toolbox [75]. This interpolation is a weighted moving average technique that uses geometric relationships between a query point and its closest subset of input samples to interpolate a value. The natural neighbor interpolation was used instead of other conventional methods such as nearest-neighbor, inverse-distance weighted averaging, and kriging because it has been proven to produce good results for unevenly distributed input datasets [76,77], which is one of the caveats when using the WS method to generate the Pareto trade-off frontiers [78,79]. Similar Pareto frontier approximation techniques have been applied in other studies [80–83].

2.5.3. Result presentation

For better representation of the results, we reported the optimal solutions on a per-liter-of-ethanol basis by dividing the landscape sums of the objective metrics by the total amount of produced ethanol, using the following equation:

$$F_i = \sum_{j=1}^{k} \frac{a_j f_j}{E} \quad (12)$$

where:

F_i = the value of objective i per liter of ethanol produced (i = feedstock-delivered costs, GHG emissions, or N leaching),
j = the j^{th} farm within the landscape,
k = number of chosen farms in the landscape (k ≤ NF),
a_j = the area of the j^{th} farm (ha),
f_j = the value of objective i per hectare basis of the j^{th} farm within the landscape,
E = the total amount of ethanol produced (E = 1.51×10^8 L year^{-1}).

3. Results and discussion

3.1. Ecosystem responses to changes in management practices

Our results showed various trade-offs among ecosystem function indicators induced by changes in management practices (Fig. 3). Increasing N fertilization resulted in a win-lose situation between improving corn grain, harvested stover, and soil organic carbon (SOC) stock and increasing soil N_2O emissions and N leaching where N fertilizer rates were moderate to low ($\leq$110 kg N ha^{-1}). However, as the N fertilizer rate exceeded 110 kg N ha^{-1}, this trade-off became a lose-lose situation where the effects of additional N fertilizer on corn grain,

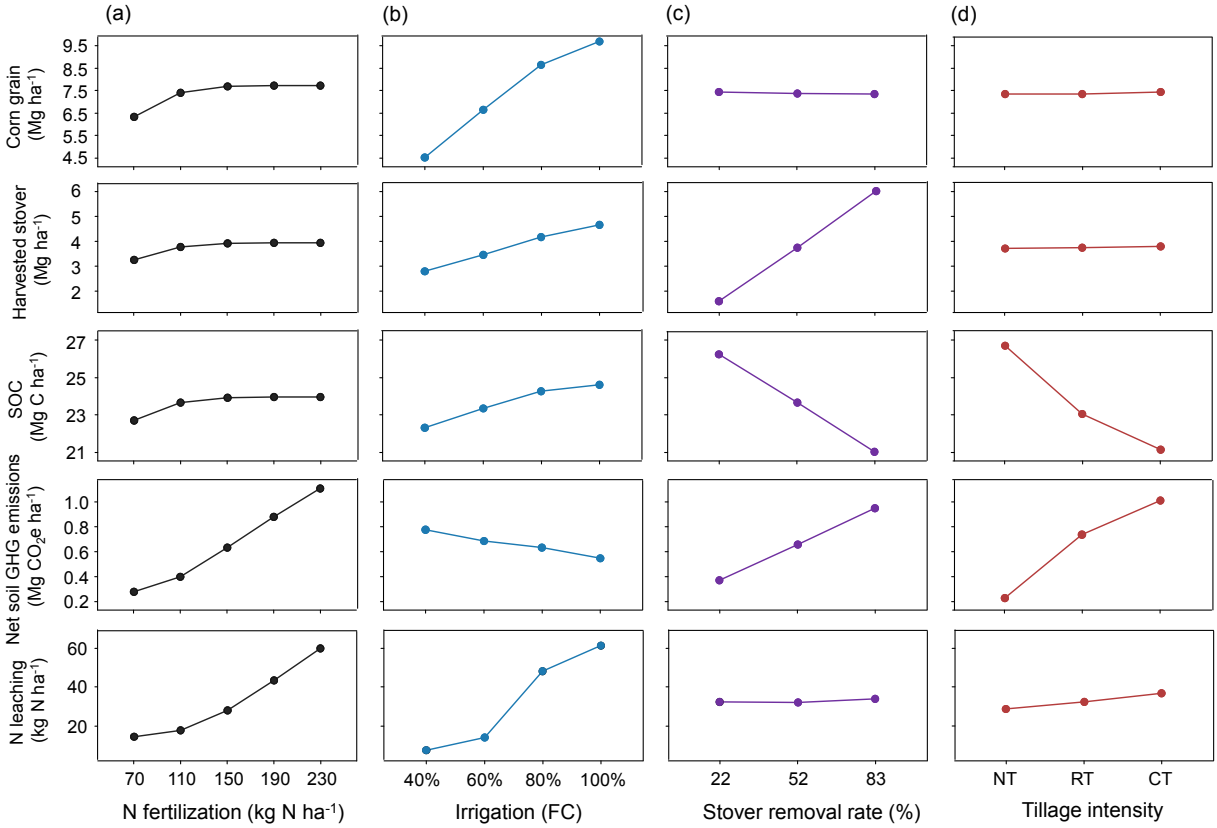

Fig. 3. Changes in ecosystem parameters by (a) N fertilizer rates averaged across other management practices; (b) irrigation rates averaged across other management practices; (c) stover removal rates averaged across other management practices; (d) tillage intensity averaged across other management practices. FC is soil-specific field capacity. Soil organic carbon (SOC) is reported for top soil (0–20 cm) at the end of the 30-year simulation period. Corn grain and corn stover are reported as 30-year average of dry matter at harvest. Net soil GHG emissions are the 30-year average of all soil-related CO_2e emissions, including soil C stock change. N leaching is the 30-year average of nitrogen that leached out of the soil profile.

harvested stover, and SOC stock diminished and the negative impacts of N fertilization on elevating soil emissions and N leaching linearly increased. While higher irrigation intensified N leaching, the positive impacts of irrigation on biomass production increased SOC stocks due to higher C inputs from residues. This net soil C stock increase (representing CO_2 removal) offset a large portion of soil N_2O emissions. The increases in stover removal rate or tillage intensity reduced C inputs to soil resulting in lower SOC stocks and higher soil emissions. Corn grain yield and N leaching were quite unresponsive to changes in stover removal rate and tillage intensity. The complex interactions between ecosystem parameters and management practices illustrated the necessity of the subsequent optimizations of the landscape design for multi-criteria decision-making.

3.2. Corner solutions for dual versus single feedstocks for ethanol production

Utilizing both corn grain and stover for ethanol production resulted in lower minimum feedstock-delivered costs, GHG emissions, and N leaching footprints of ethanol at the refinery gate than those of single feedstocks (Fig. 4). Compared to the dual feedstock ethanol, grain-based ethanol was 1.3 times higher in feedstock-delivered costs, 1.2 times higher in GHG emissions, and 12 times higher in N leaching. Similarly, stover-based ethanol had the refinery-gate footprints of 1.9, 5.3, and 283 times higher that dual feedstock ethanol, in terms of feedstock-delivered costs, GHG emissions, and N leaching, respectively. Such increases in feedstock-delivered costs and environmental footprints were mainly due to higher required area for feedstock production and the intensification of management practices (Table 5).

When comparing across the objective scenarios, we found that the minimum feedstock-delivered costs (minCost) was achieved with higher average management inputs but reduced feedstock area (Table 5). This was because the fixed costs increased with increasing number of feedstock sites. To attain minimum GHG emissions (minGHG), lower N fertilizer, irrigation, and stover removal rates were applied to reduce farm machinery emissions and increase the C credits from SOC stock change. This led to a substantial expansion of feedstock area and a higher proportion of grain-based ethanol. To minimize N leaching (minNL), the model used low N fertilizer and irrigation rates to reduce N leaching sources while increasing stover removal rates to curtail the required feedstock area. No-till was dominantly applied as the optimum tillage type in all corner scenarios with 100% of landscape under minCost and minGHG scenarios and 88–95% under minNL scenarios. The spatial configurations of optimum management practices for each corn field in the landscape under the corner objective scenarios are provided in Supplementary Materials S3.

3.3. Pareto trade-off surface for three design objectives

The Pareto surface for simultaneous minimization of feedstock-delivered costs, farm-to-refinery GHG emissions, and N leaching exhibits non-smooth patterns (Fig. 5a). The surface's borders define the Pareto frontiers representing trade-offs between each pair of the design objectives (i.e., scenarios where one of the weighting coefficients is zero), including Pareto frontiers between feedstock-delivered costs and farm-to-refinery GHG emissions (Cost vs. GHG) (Fig. 5b), Pareto frontiers between feedstock-delivered costs and N leaching (Cost vs. NL) (Fig. 5c), and Pareto frontiers between farm-to-refinery GHG emissions and N leaching (GHG vs. NL) (Fig. 5d). We found that minimum feedstock-delivered costs came with maximum N leaching while minimum

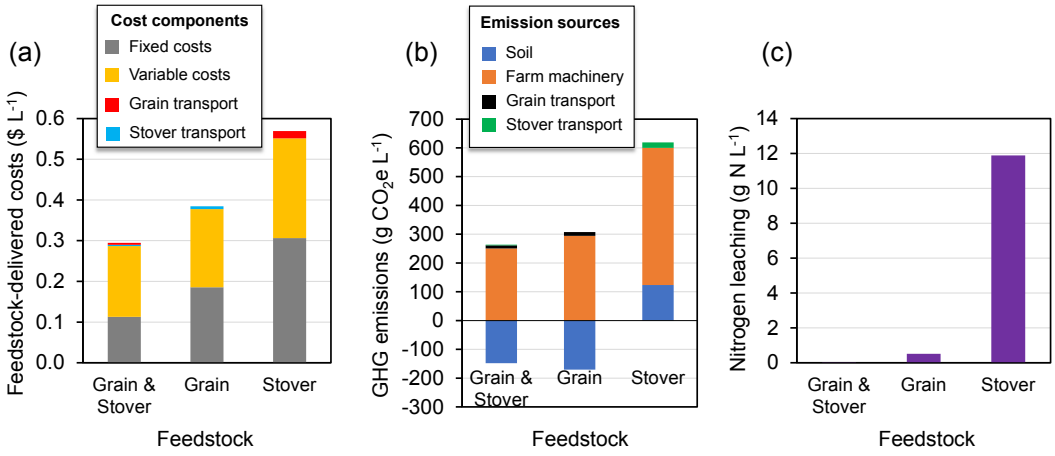

Fig. 4. Comparison of the corner solutions between dual and single feedstocks for ethanol production. These solutions corresponded to the situations where single objectives were considered in the optimization. (a) Minimum feedstock-delivered costs (minCost scenario); (b) Minimum GHG emissions (minGHG scenario); and (c) Minimum N leaching (minNL scenario).

N leaching corresponded to maximum GHG emissions. This was due to the decrease in required feedstock area and the intensification of management inputs. Our results showed that the feedstock-delivered costs ranged from \$0.29 L^{-1} to \$0.47 L^{-1}, farm-to-refinery GHG emissions ranged from 0.04 to 8.77 (g N L^{-1}), and N leaching ranged 116–274 (g CO2e L^{-1}). However, the long tails associated with minCost, minNL, and minGHG scenarios suggested that the marginal decreases of feedstock-delivered costs (below \$0.31 L^{-1}), N leaching (below 0.44 g N L^{-1}), and GHG emissions (below 125 g CO_2e L^{-1}) resulted in extreme trade-offs among the design objectives. The optimal break-even prices of biofuel feedstocks at the refinery gate ranged from \$140–\$215 per Mg d.m of corn grain and \$87 – \$117 per Mg d.m of corn stover (Supplementary Materials S4). This corresponded to (−22.2%)–19.4% and 24.3% – 67.1% increases compared to the market values used in this analysis for corn grain and stover, respectively.

We further examined the internalization of SC-CO_2 and SC-NL as a mean to reduce GHG emissions and N leaching for biofuel supply chains. The literature estimates of social costs of GHG emissions and N leaching varied greatly with SC-CO_2 ranging from \$39 to \$220 per Mg CO_2e [84,85,72,86,87] and SC-NL ranging from < \$1 to \$56 per kg N [73,88–90]. We compared the solutions for the lower bound (w_1 = 1, SC-CO_2 = \$39 Mg^{-1}, SC-NL = \$1 kg^{-1}) and upper bound (w_1 = 1, SC-CO_2 = \$220 Mg^{-1}, SC-NL = \$56 kg^{-1}) scenarios with that of the control scenario (minCost: w_1 = 1, SC-CO_2 = \$0 Mg^{-1}, SC-NL = \$0 kg^{-1}) (Fig. 5). Our result showed that accounting for social costs of GHG emissions and N leaching in the feedstock landscape planning would reduce the GHG emission footprints by 2.8–11.4% and N leaching footprints by 29.3–96.4% for lower and upper bound scenarios, respectively. However, this would increase the feedstock-delivered costs by 0.7–18%.

3.4. Optimum management practices

The modulation of management practices, feedstock area, and corn grain ethanol percentage to attain optimal solutions are given in Fig. 6. In general, our model maintained minimal stover removal rate while lowering N fertilization and irrigation to minimize GHG emissions whereas it retained minimal N fertilization and irrigation while increasing stover removal (thus reducing feedstock area) to minimize N leaching. To minimize feedstock-delivered costs, our model attempted to reduce the feedstock area by orchestrating the rates of change among different management practices. For example, we observed consistent increases in N fertilization, irrigation, and stover harvest when shifting from minNL to minCost scenarios and periodic adjustments of N fertilization, irrigation, and stover harvest rates moving along the Cost vs. GHG Pareto frontier. The minimum feedstock area required for 1.51×10^8 L $year^{-1}$ was 19,629 ha (35% of total study area) corresponding to the minCost solution while maximum feedstock area was 47,324 ha (85% of total study area) obtained at a solution on the NL vs. GHG Pareto frontier. This was the situation where reducing N leaching and GHG emissions were equally weighted and thus the model sustained the lowest production level. The percentage of grain-based ethanol strongly correlated with stover removal (r = −0.98) and

Table 5
Landscape average of management inputs for the corner solutions.

Single objective scenario	Feedstock type	Landscape average* of			Percentage of feedstock area (%)	Grain-based ethanol (%)
		N fertilizer (kg N ha^{-1})	Irrigation (cm $year^{-1}$)	Stover removal rate (%)		
minCost	Grain & Stover	150	45	83	35.4	61
	Grain	150	44	50	58.3	100
	Stover	150	42	83	96.1	0
minGHG	Grain & Stover	88	29	22	71.1	85
	Grain	91	30	22	82.0	100
	Stover	135	41	83	100.0	0
minNL	Grain & Stover	80	23	80	62.1	59
	Grain	94	24	42	99.4	100
	Stover	146	40	83	100.0	0

Note: * To calculate the landscape average of a scenario, each field was weighted by its area and the weighted sum was divided by the corresponding feedstock area.

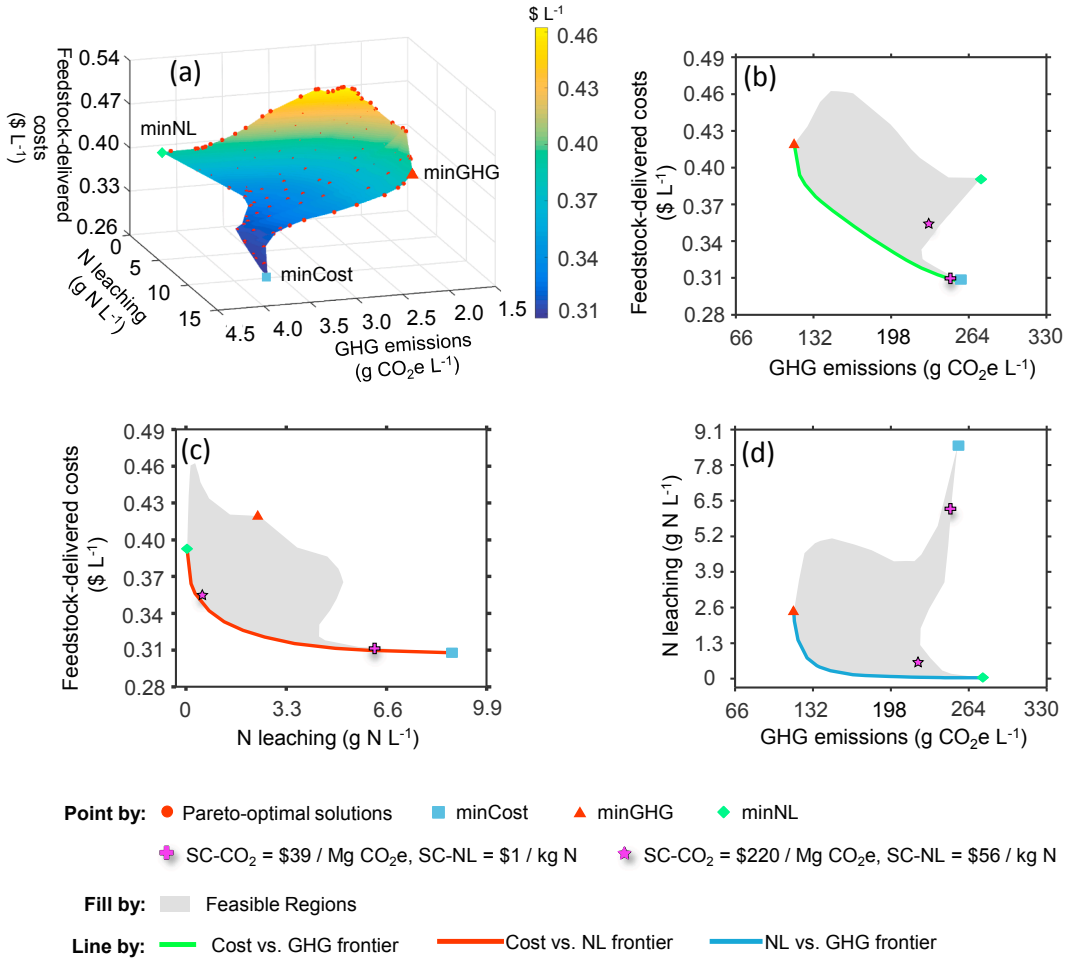

Fig. 5. Pareto surface for trade-offs among three design objectives. (a) 3D Pareto surface; (b) 2D projection of the 3D Pareto surface highlighting trade-off between feedstock-delivered costs and farm-to-refinery GHG emissions, (c) 2D projection of the 3D Pareto surface highlighting trade-off between feedstock-delivered costs and N leaching, (d) 2D projection of the 3D Pareto surface highlighting trade-off between N leaching and farm-to-refinery GHG emissions. The colored points show Pareto-optimal solutions for scenarios where different social cost of CO_2 (SC-CO_2) and social cost of N leaching (SC-NL) were used as weighting coefficients in the objective functions (Eq. (1)).

ranged from 59% to 85% of the total 1.51×10^8 L year^{-1}.

3.5. Emission credits from ethanol production

Based on the Pareto-optimal solutions, our results estimated an average reduction of 51% and 77% in life-cycle GHG emissions as compared to conventional gasoline for the production and utilization of grain-based and stover-based ethanol, respectively (Fig. 7). These corresponded to the avoided CO_2e emissions of 0.44 Mg CO_2e Mg^{-1} for corn grain and 0.54 Mg CO_2e Mg^{-1} for corn stover used as feedstock for biofuels (Fig. 7b), which outweighed those achieved by soil SOC increases as compared to BAU scenario (Fig. 7c). We did not consider the GHG credits from ethanol production and utilization in the calculation of farm-to refinery GHG since that requires extrapolations beyond the boundary of our analysis. However, if such GHG credits were applied in the analysis, our model would favor the intensification of management

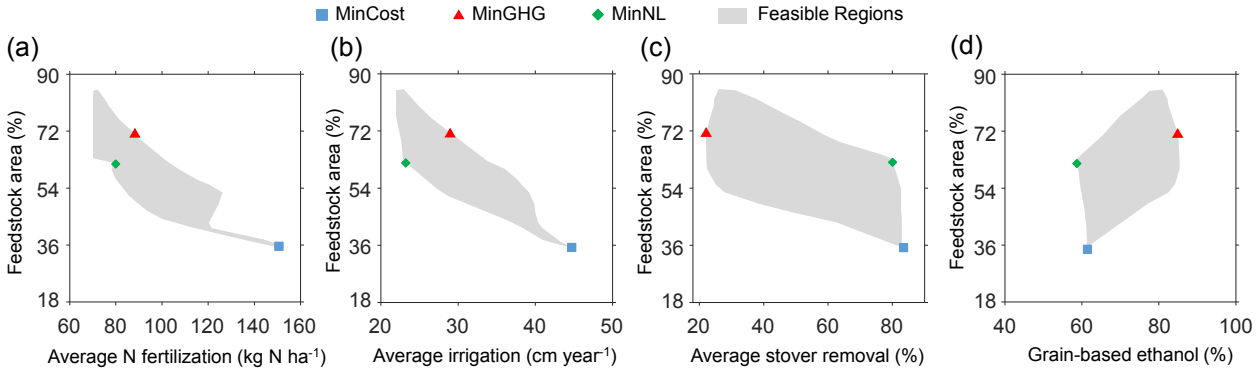

Fig. 6. Optimal management corresponding to solutions on the Pareto surface. This figure plots the percentage of feedstock area (of the total 55,401 ha) on the y-axes against (a) average N fertilization, (b) average irrigation, (c) grain-based ethanol percentage.

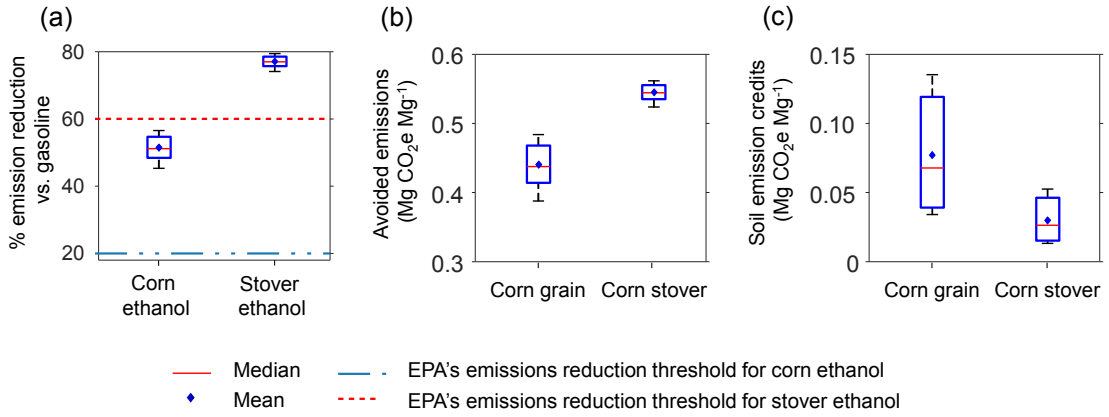

Fig. 7. Emission-related results for Pareto-optimal solutions. (a) Emissions reductions of grain- and stover-based ethanol as compared to conventional gasoline. (b) Avoided emissions from the production and utilization of ethanol attributed to corn grain and corn stover. (c) Emission credits due to increases in SOC stock as compared to the business-as-usual scenario attributed to corn grain and corn stover.

inputs and stover removal rates to maximize feedstock yields. This, in turn, would substantially decrease SOC stocks and might result in potential reductions of long-term soil health.

3.6. Effects of social costs on objective trade-offs

The effects of SC-CO_2 and SC-NL on the trade-offs between each pair of the design objectives along the Pareto frontiers (a.k.a., the borders of the Pareto surface) are illustrated in Fig. 8. We did not present such effects for data on the Pareto surface since they required a higher dimensional interpolation of the relationships among the weighting coefficient for feedstock-delivered costs (w_1), SC-CO_2, and SC-NL. The generation of GHG vs. NL frontier required varying both SC-CO_2 and SC-NL in the integrated objective function, thus the SC-CO_2/SC-NL ratio was used in the x-axis (Fig. 8c). We limited SC-CO_2 between \$0 and \$5000 per Mg CO_2e, SC-NL between \$0 and \$500 per kg N, and the ratio between 0 and 600 to highlight the most dynamic variations in the design objective values. Our result indicated that the feedstock landscape design was more sensitive to changes of SC-CO_2 between \$400 and \$800 per Mg CO_2e (Fig. 8a), changes of SC-NL below \$50 per kg N (Fig. 8b), and changes in SC-CO_2/SC-NL ratio below 350 (Fig. 8c).

4. Discussion

Our analysis could provide valuable insights to support decision-making in designing sustainable biomass supply chains. For example, the results of our analysis could be used to inform Front Range Energy on (1) how much land they should use for feedstock production; (2) where in the landscape to produce the feedstocks; (3) how much of first- and second-generation biofuels to produce; (4) what the optimum management practices (e.g., rates of N fertilization, irrigation, stover removal, and tillage intensity) they should recommend to apply for each corn field; (5) how the decision-making could affect the economic and environmental footprints of the produced ethanol; and (6) how external drivers such as potential policies on social costs might affect the feedstocks production for biofuels. We believe such insights could improve the efficiency of biomass supply chains, making large-scale production and use of biofuels more viable and sustainable.

While our study demonstrated a simple tri-objective optimization problem for a single cropping system, the approach and the resulting model would be equally applicable for more complex problems, such as those involving broader system boundaries, more optimization objectives and constraints, multiple cropping systems, and/or variations in economic variables. However, as implied by our analysis, optimizations that consider broader system boundaries and/or include GHG credits from the production and use of biofuels should pay more attention to long-term soil's health, especially soil organic carbon stock. Such optimizations should be coupled with a SOC objective or apply a critical SOC threshold as a constraint to ensure ecosystem sustainability.

Despite the potential advantages of our approach, we do realize some caveats in our methodology. For instance, ecosystem modeling expertise and advanced computational infrastructure are often required to carry out this type of analysis. Besides, our discrete optimization approach is computationally expensive since it requires the use of complex simulation models (e.g., DayCent, Ag-EcoSOpt and GREET) to quantify the management-induced ecosystem responses as input for the subsequent optimizations. Furthermore, the generation of Pareto optimum set was time intensive due to the iterative optimization of the scalarized multi-objective problems. These issues are magnified when finer landscape exploratory simulations or more Pareto optimum points are desired to better approximate global optimum solutions. These challenges could make our approach impractical in most institutional contexts that require timely analysis to support rational decision making. A possible solution for this problem is to use meta-modeling

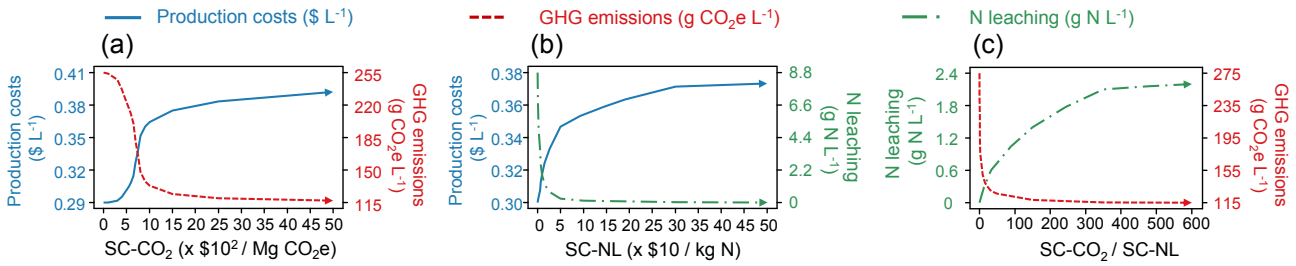

Fig. 8. Effects of social costs of carbon and N leaching on design objective trade-offs along Pareto frontiers. (a) Effect of changes in social costs of carbon on feedstock-delivered costs and GHG emissions. (b) Effect of changes in social costs of N leaching on feedstock-delivered costs and N leaching. (c) Effect of changes in social costs of carbon and N leaching ratio on N leaching and GHG emissions.

techniques to create simplified surrogate models to reduce simulation time and data storage requirement [91].

The use of the weighted sum method for Pareto frontier generation is often accompanied by some of its inherent drawbacks. For example, it is unable to find solutions in non-convex regions and rarely produces an even spread of Pareto points with constant incremental steps of the weighting coefficients [78]. Since our scope was to approximate the extent of the Pareto surface, we overcame these drawbacks by formulating our problem with linear programming to ensure convexity, roughly estimating the borders of the Pareto surface by iteratively solving bi-objective optimizations and using natural neighbor interpolation method to handle the unevenly distributed Pareto points. However, for more complex multi-objective problems with potential non-linear objectives and constraints, other advanced methods should be used such as adaptive weighted sum [92], modified normal boundary intersection, and modified normal constraint [79]. Last but not least, since we only approximated the extent of the Pareto surface, we did not concentrate on the refinement of Pareto optimal solutions on the produced Pareto surface. Therefore, our method might not guarantee the Pareto-optimal property of many interpolated data points. The fine-tuning of the Pareto front and Pareto surface approximation, especially for nonconvex optimization problems with more than two objectives, can be done with more advanced algorithms such as adaptive weighted sum [92], modified normal boundary intersection, modified normal constraint [79], PAINT [93], and Interactive Decision Maps [94].

5. Conclusion

In this study, we demonstrated a high spatial resolution and multi-objective optimization of feedstock landscape design for a hybrid first- and second-generation biofuel supply chain. A discrete optimization approach was used in junction with the life cycle optimization framework to optimize system outcomes for the cultivation of corn grain and corn stover for ethanol production at Front Range Energy biorefinery (FRE), Windsor, Colorado, USA. The analysis was formulated as a tri-objective linear programming problem, including minimization of feedstock-delivered costs, farm-to-refinery greenhouse gas emissions, and nitrogen leaching, subject to meeting feedstock demand for the ethanol production capacity of 1.51×10^8 L year^{-1} (~40 million U.S. gallons per year). In particular, we addressed the questions of (1) how much land should be used for feedstock production; (2) where to produce the feedstocks; (3) how much of corn grain and corn stover to produce; and (4) what the optimum management practices (e.g., rates of N fertilization, irrigation, stover removal, and tillage intensity) are to apply for each corn field in the chosen landscape. Our results showed a broad win-lose Pareto surface among the three design objectives and various modulating patterns of the required feedstock area, management input investments, and grain-based and stover-based ethanol ratio associating with optimum solutions on the Pareto surface. Although our model relies heavily on ecosystem modeling expertise and advanced computational infrastructure, it could be a useful tool for solving many complex resource management problems that require detailed trade-off analysis of different objectives at high spatial resolutions. We also believe that the approach and modeling platform employed in this site-specific study would be equally applicable for other problems to support environmentally-conscious decision making in sustainable resource management for biofuel supply chains.

Acknowledgements

The work was supported by a USDA/NIFA project (grant# 2011-67009-30083) “Decision support tool for integrated biofuel greenhouse gas emission footprints”, the Fulbright Vietnam scholarship, the Multidisciplinary Approaches to Sustainable BioEnergy PhD program funded by the United States National Science Foundation, Hue University of Agriculture and Forestry, Vietnam (HUAF), and Shell Technology Center Houston, USA. The authors thank colleagues at the Natural Resource Ecology Laboratory (NREL) for assistance with simulation modeling and Dr. Christian Davies at Shell Technology Center Houston for data sources.

Appendix A. Supplementary material

Supplementary data to this article can be found online at https://doi.org/10.1016/j.apenergy.2019.01.117.

References

[1] EPA-RFS2. Renewable fuel standard (RFS2): final rule (no. legal authority: 42 U.S.C. §7545). United States Environmental Protection Agency; 2010.
[2] Searchinger T, Heimlich R, Houghton RA, Dong F, Elobeid A, Fabiosa J, et al. Use of U.S. croplands for biofuels increases greenhouse gases through emissions from land-use change. Science 2008;319:1238–40. https://doi.org/10.1126/science.1151861.
[3] Gnansounou E, Dauriat A, Villegas J, Panichelli L. Life cycle assessment of biofuels: energy and greenhouse gas balances. Bioresour Technol 2009;100:4919–30. https://doi.org/10.1016/j.biortech.2009.05.067.
[4] Farrell AE, Plevin RJ, Turner BT, Jones AD, O’Hare M, Kammen DM. Ethanol can contribute to energy and environmental goals. Science 2006;311:506–8. https://doi.org/10.1126/science.1121416.
[5] Reijnders L, Huijbregts MAJ. Life cycle greenhouse gas emissions, fossil fuel demand and solar energy conversion efficiency in European bioethanol production for automotive purposes. J Clean Prod 2007;15:1806–12. https://doi.org/10.1016/j.jclepro.2006.05.007.
[6] Awudu I, Zhang J. Uncertainties and sustainability concepts in biofuel supply chain management: a review. Renew Sustain Energy Rev 2012;16:1359–68. https://doi.org/10.1016/j.rser.2011.10.016.
[7] Yue D, You F, Snyder SW. Biomass-to-bioenergy and biofuel supply chain optimization: overview, key issues and challenges. Comput Chem Eng, Selected papers from ESCAPE-23 (European Symposium on Computer Aided Process Engineering – 23), 9–12 June 2013 Lappeenranta, Finland 2014;66:36–56. https://doi.org/10.1016/j.compchemeng.2013.11.016.
[8] Mele FD, Kostin AM, Guillén-Gosálbez G, Jiménez L. Multiobjective model for more sustainable fuel supply chains. A case study of the sugar cane industry in Argentina. Ind Eng Chem Res 2011;50:4939–58. https://doi.org/10.1021/ie101400g.
[9] Corsano G, Vecchietti AR, Montagna JM. Optimal design for sustainable bioethanol supply chain considering detailed plant performance model. Comput Chem Eng Energy Sustain 2011;35:1384–98. https://doi.org/10.1016/j.compchemeng.2011.01.008.
[10] Akgul O, Zamboni A, Bezzo F, Shah N, Papageorgiou LG. Optimization-based approaches for bioethanol supply chains. Ind Eng Chem Res 2011;50:4927–38. https://doi.org/10.1021/ie101392y.
[11] Čuček L, Lam HL, Klemeš JJ, Varbanov PS, Kravanja Z. Synthesis of regional networks for the supply of energy and bioproducts. Clean Technol Environ Policy 2010;12:635–45. https://doi.org/10.1007/s10098-010-0312-6.
[12] Huang Y, Chen C-W, Fan Y. Multistage optimization of the supply chains of biofuels. Transp Res Part E Logist Transp Rev 2010;46:820–30. https://doi.org/10.1016/j.tre.2010.03.002.
[13] Santibañez-Aguilar JE, González-Campos JB, Ponce-Ortega JM, Serna-González M, El-Halwagi MM. Optimal planning of a biomass conversion system considering economic and environmental aspects. Ind Eng Chem Res 2011;50:8558–70. https://doi.org/10.1021/ie102195g.
[14] Giarola S, Zamboni A, Bezzo F. Spatially explicit multi-objective optimisation for design and planning of hybrid first and second generation biorefineries. Comput Chem Eng, Energy Systems Engineering 2011;35:1782–97. https://doi.org/10.1016/j.compchemeng.2011.01.020.
[15] Akgul O, Shah N, Papageorgiou LG. An optimisation framework for a hybrid first/second generation bioethanol supply chain. Comput Chem Eng, European Symposium of Computer Aided Process Engineering 2012;21(42):101–14. https://doi.org/10.1016/j.compchemeng.2012.01.012.
[16] Gonela V, Zhang J, Osmani A. Stochastic optimization of sustainable industrial symbiosis based hybrid generation bioethanol supply chains. Comput Ind Eng 2015;87:40–65. https://doi.org/10.1016/j.cie.2015.04.025.
[17] Mutenure M, Čuček L, Egieya J, Isafiade AJ, Kravanja Z. Optimization of bioethanol and sugar supply chain network: a South African case study. Clean Technol Environ Policy 2018;20:925–48. https://doi.org/10.1007/s10098-018-1535-1.
[18] Yu TE, Wang Z, English BC, Larson JA. Designing a dedicated energy crop supply system in Tennessee: a multiobjective optimization analysis. J Agric Appl Econ 2014;46:357.
[19] Lautenbach S, Volk M, Strauch M, Whittaker G, Seppelt R. Optimization-based trade-off analysis of biodiesel crop production for managing an agricultural catchment. Environ Model Softw 2013;48:98–112. https://doi.org/10.1016/j.envsoft.2013.06.006.
[20] Parish ES, Hilliard MR, Baskaran LM, Dale VH, Griffiths NA, Mulholland PJ, et al. Multimetric spatial optimization of switchgrass plantings across a watershed. Biofuels Bioprod Biorefin 2012;6:58–72. https://doi.org/10.1002/bbb.342.
[21] Zhang X, Izaurralde RC, Manowitz D, West TO, Post WM, Thomson AM, et al. An integrative modeling framework to evaluate the productivity and sustainability of

biofuel crop production systems. GCB Bioenergy 2010;2:258–77. https://doi.org/10.1111/j.1757-1707.2010.01046.x.
[22] Nguyen TH, Cook M, Field JL, Khuc QV, Paustian K. High-resolution trade-off analysis and optimization of ecosystem services and disservices in agricultural landscapes. Environ Model Softw 2018;107:105–18. https://doi.org/10.1016/j.envsoft.2018.06.006.
[23] Field JL, Evans SG, Marx E, Easter M, Adler PR, Dinh T, et al. High-resolution techno–ecological modelling of a bioenergy landscape to identify climate mitigation opportunities in cellulosic ethanol production. Nat Energy 2018;3:211. https://doi.org/10.1038/s41560-018-0088-1.
[24] Sahoo K, Mani S, Das L, Bettinger P. GIS-based assessment of sustainable crop residues for optimal siting of biogas plants. Biomass Bioenergy 2018;110:63–74. https://doi.org/10.1016/j.biombioe.2018.01.006.
[25] Davis SC, Boddey RM, Alves BJR, Cowie AL, George BH, Ogle SM, et al. Management swing potential for bioenergy crops. GCB Bioenergy 2013;5:623–38. https://doi.org/10.1111/gcbb.12042.
[26] Nguyen TH, Williams S, Paustian K. Impact of ecosystem carbon stock change on greenhouse gas emissions and carbon payback periods of cassava-based ethanol in Vietnam. Biomass Bioenergy 2017;100:126–37. https://doi.org/10.1016/j.biombioe.2017.02.009.
[27] Kragt ME, Robertson MJ. Quantifying ecosystem services trade-offs from agricultural practices. Ecol Econ 2014;102:147–57. https://doi.org/10.1016/j.ecolecon.2014.04.001.
[28] Balbi S, del Prado A, Gallejones P, Geevan CP, Pardo G, Pérez-Miñana E, et al. Modeling trade-offs among ecosystem services in agricultural production systems. Environ Model Softw 2015;72:314–26. https://doi.org/10.1016/j.envsoft.2014.12.017.
[29] Parton WJ, Schimel DS, Ojima DS, Cole CV. A general model for soil organic matter dynamics: sensitivity to litter chemistry, texture and management. Soil Science Society of America Inc.; 1994. p. 147–67.
[30] Del Grosso SJ, Parton WJ, Mosier AR, Ojima DS, Kulmala AE, Phongpan S. General model for N_2O and N_2 gas emissions from soils due to dentrification. Glob Biogeochem Cycles 2000;14:1045–60. https://doi.org/10.1029/1999GB001225.
[31] Li C, Frolking S, Frolking TA. A model of nitrous oxide evolution from soil driven by rainfall events: 1. Model structure and sensitivity. J Geophys Res Atmos 1992;97:9759–76. https://doi.org/10.1029/92JD00509.
[32] Coleman K, Jenkinson DS. RothC-26.3 – a model for the turnover of carbon in soil. In: Powlson DS, Smith P, Smith JU, editors. Evaluation of soil organic matter models, NATO ASI series. Berlin, Heidelberg: Springer; 1996. p. 237–46.
[33] Keating BA, Carberry PS, Hammer GL, Probert ME, Robertson MJ, Holzworth D, et al. An overview of APSIM, a model designed for farming systems simulation. Eur J Agron Modelling Cropping Systems: Science, Software and Applications 2003;18:267–88. https://doi.org/10.1016/S1161-0301(02)00108-9.
[34] Paustian K, Ogle SM, Conant RT. Quantification and decision support tools for US agricultural soil carbon sequestration. Handbook of climate change and agroecosystems, ICP series on climate change impacts, adaptation, and mitigation. Imperial College Press; 2010. p. 307–41.
[35] Zamboni A, Bezzo F, Shah N. Spatially explicit static model for the strategic design of future bioethanol production systems. 2. Multi-objective environmental optimization. Energy Fuels 2009;23:5134–43. https://doi.org/10.1021/ef9004779.
[36] Bernardi A, Giarola S, Bezzo F. Optimizing the economics and the carbon and water footprints of bioethanol supply chains. Biofuels Bioprod Biorefin 2012;6:656–72. https://doi.org/10.1002/bbb.1358.
[37] Yue D, Kim MA, You F. Design of sustainable product systems and supply chains with life cycle optimization based on functional unit: general modeling framework, mixed-integer nonlinear programming algorithms and case study on hydrocarbon biofuels. ACS Sustain Chem Eng 2013;1:1003–14. https://doi.org/10.1021/sc400080x.
[38] You F, Tao L, Graziano DJ, Snyder SW. Optimal design of sustainable cellulosic biofuel supply chains: multiobjective optimization coupled with life cycle assessment and input–output analysis. AIChE J 2012;58:1157–80. https://doi.org/10.1002/aic.12637.
[39] Bernardi A, Giarola S, Bezzo F. Spatially explicit multiobjective optimization for the strategic design of first and second generation biorefineries including carbon and water footprints. Ind Eng Chem Res 2013;52:7170–80. https://doi.org/10.1021/ie302442j.
[40] Čuček L, Klemeš JJ, Kravanja Z. A review of footprint analysis tools for monitoring impacts on sustainability. J Clean Prod, Recent Cleaner Production Advances in Process Monitoring and Optimisation 2012;34:9–20. https://doi.org/10.1016/j.jclepro.2012.02.036.
[41] Mesinger F, DiMego G, Kalnay E, Mitchell K, Shafran PC, Ebisuzaki W, et al. North American regional reanalysis. Bull Am Meteorol Soc 2006;87:343–60. https://doi.org/10.1175/BAMS-87-3-343.
[42] Finkbeiner M, Inaba A, Tan R, Christiansen K, Klüppel H-J. The new international standards for life cycle assessment: ISO 14040 and ISO 14044. Int J Life Cycle Assess 2006;11:80–5. https://doi.org/10.1065/lca2006.02.002.
[43] Wang M, Han J, Dunn JB, Cai H, Elgowainy A. Well-to-wheels energy use and greenhouse gas emissions of ethanol from corn, sugarcane and cellulosic biomass for US use. Environ Res Lett 2012;7:045905. https://doi.org/10.1088/1748-9326/7/4/045905.
[44] Wang Z, Dunn JB, Han J, Wang MQ. Influence of corn oil recovery on life-cycle greenhouse gas emissions of corn ethanol and corn oil biodiesel. Biotechnol Biofuels 2015;8:178. https://doi.org/10.1186/s13068-015-0350-8.
[45] Thompson J, Tyner WE. Corn stover for bioenergy production: cost estimates and farmer supply response. Purdue extension renewable energy series. Purdue Extension, Purdue University; 2011.
[46] UChicago Argonne. The greenhouse gases, regulated emissions, and energy use in transportation model. Argonne National Laboratory; 2015.
[47] Mitchell S, Consulting SM, Dunning I. PuLP: a linear programming toolkit for Python. Auckland, New Zealand: The University of Auckland; 2011.
[48] IBM®, IBM ILOG CPLEX optimization studio. IBM®; 2017.
[49] Parton WJ, Hartman M, Ojima D, Schimel D. DAYCENT and its land surface submodel: description and testing. Glob Planet Change 1998;19:35–48. https://doi.org/10.1016/S0921-8181(98)00040-X.
[50] Del Grosso S, Ojima D, Parton W, Mosier A, Peterson G, Schimel D. Simulated effects of dryland cropping intensification on soil organic matter and greenhouse gas exchanges using the DAYCENT ecosystem model. Environ Pollut Barking Essex 1987 2002;116(Suppl 1):S75–83.
[51] Delgrosso S, Mosier A, Parton W, Ojima D. DAYCENT model analysis of past and contemporary soil NO and net greenhouse gas flux for major crops in the USA. Soil Tillage Res. 2005;83:9–24. https://doi.org/10.1016/j.still.2005.02.007.
[52] Del Grosso SJ, Halvorson AD, Parton WJ. Testing DAYCENT model simulations of corn yields and nitrous oxide emissions in irrigated tillage systems in Colorado. J Environ Qual 2008;37:1383. https://doi.org/10.2134/jeq2007.0292.
[53] Del Grosso SJ, Parton WJ, Ojima DS, Keough CA, Riley TH, Mosier AR. DAYCENT simulated effects of land use and climate on county level N loss vectors in the USA. Publ. USDA-ARSUNL Fac. 255; 2008.
[54] Kim S, Dale BE, Jenkins R. Life cycle assessment of corn grain and corn stover in the United States. Int J Life Cycle Assess 2009;14:160–74. https://doi.org/10.1007/s11367-008-0054-4.
[55] David MB, Grosso SJD, Hu X, Marshall EP, McIsaac GF, Parton WJ, et al. Modeling denitrification in a tile-drained, corn and soybean agroecosystem of Illinois, USA. Biogeochemistry 2008;93:7–30. https://doi.org/10.1007/s10533-008-9273-9.
[56] US EPA CCD. Inventory of U.S. greenhouse gas emissions and sinks: 1990–2013 (collections & list, no. 430-R-14–003); 2015.
[57] Ogle SM, Breidt FJ, Easter M, Williams S, Killian K, Paustian K. Scale and uncertainty in modeled soil organic carbon stock changes for US croplands using a process-based model. Glob Change Biol 2010;16:810–22. https://doi.org/10.1111/j.1365-2486.2009.01951.x.
[58] ERS-ARMS. Farm financial and crop production practices. Economic Research Service, United States Department of Agriculture; 2010.
[59] Halvorson AD, Mosier AR, Reule CA, Bausch WC. Nitrogen and tillage effects on irrigated continuous corn yields. Agron J 2006;98:63. https://doi.org/10.2134/agronj2005.0174.
[60] Muth Jr DJ, Bryden KM, Nelson RG. Sustainable agricultural residue removal for bioenergy: a spatially comprehensive US national assessment. Appl Energy, Special Issue on Advances in sustainable biofuel production and use - XIX International Symposium on Alcohol Fuels - ISAF 2013;102:403–17. https://doi.org/10.1016/j.apenergy.2012.07.028.
[61] Vadas PA, Digman MF. Production costs of potential corn stover harvest and storage systems. Biomass Bioenergy 2013;54:133–9. https://doi.org/10.1016/j.biombioe.2013.03.028.
[62] Russell J, Dalsted N, Tranel J, Young RB, Seyler J. Custom rates for Colorado farms & ranches in 2015. Agriculture & Business Management Notes, Colorado State University Extension; 2016.
[63] Ibendahl G, O'Brien DM, Duncan. Center-pivot-irrigated corn cost-return budget in North Central Kansas (No. MF2601). Department of Agricultural Economics, Kansas State University; 2015.
[64] Gesch RW, Archer DW, Forcella F. Rotational Effects of cuphea on corn, spring wheat, and soybean. Agron J 2010;102:145. https://doi.org/10.2134/agronj2009.0215.
[65] Eve M, Pape D, Flugge M, Steele R, Man D, Gilbert M, et al. Quantifying greenhouse gas fluxes in agriculture and forestry: methods for entity-scale inventory (no. technical bulletin number 1939). Washington, DC: U.S. Department of Agriculture, Office of the Chief Economist; 2014.
[66] IPCC. 2006 IPCC guidelines for national greenhouse gas inventories. Hayama, Japan: Institute for Global Environmental Strategies; 2006.
[67] Penn State Extension. The agronomy guide 2017–2018. College of Agricultural Sciences, The Pennsylvania State University; 2017.
[68] Rathke G-W, Wienhold BJ, Wilhelm WW, Diepenbrock W. Tillage and rotation effect on corn–soybean energy balances in eastern Nebraska. Soil Tillage Res 2007;97:60–70. https://doi.org/10.1016/j.still.2007.08.008.
[69] Luo L, van der Voet E, Huppes G. An energy analysis of ethanol from cellulosic feedstock–Corn stover. Renew Sustain Energy Rev 2009;13:2003–11. https://doi.org/10.1016/j.rser.2009.01.016.
[70] Martin DL, Dorn TW, Kranz WL, Melvin SR, Corr AJ. Reducing the cost of pumping irrigation water. 2010 Central plains irrigation conference. 2010. p. 41.
[71] Fishburn PC. Additive utilities with incomplete product sets: application to priorities and assignments. Oper Res 1967;15:537–42.
[72] Tol R. The social cost of carbon. Annu Rev Resour Econ 2011;3:419–43. https://doi.org/10.1146/annurev-resource-083110-120028.
[73] Brink C, Van Grinsven H. The European Nitrogen Assessment: costs and benefits of nitrogen in the environment. Camb. Univ. Press; 2011 [chapter 22].
[74] Sibson R. A brief description of natural neighbor interpolation. John Wiley Sons N. Y., Interpolating multivariate data; 1981. p. 21–36 [chapter 2].
[75] MATLAB and Neural Network Toolbox. Neural network toolbox documentation. Natick, Massachusetts, United States: The MathWorks, Inc.; 2017.
[76] Sambridge M, Braun J, McQueen H. Geophysical parametrization and interpolation of irregular data using natural neighbours. Geophys J Int 1995;122:837–57. https://doi.org/10.1111/j.1365-246X.1995.tb06841.x.
[77] Ledoux H, Gold C. An efficient natural neighbour interpolation algorithm for geoscientific modelling. Developments in spatial data handling. Springer; 2005. p.

97–108.
[78] Marler RT, Arora JS. The weighted sum method for multi-objective optimization: new insights. Struct Multidiscip Optim 2010;41:853–62. https://doi.org/10.1007/s00158-009-0460-7.
[79] Motta R de S, Afonso SMB, Lyra PRM. A modified NBI and NC method for the solution of N-multiobjective optimization problems. Struct Multidiscip Optim 2012;46:239–59. https://doi.org/10.1007/s00158-011-0729-5.
[80] Bramanti A, Di Barba P, Farina M, Savini A. Combining response surfaces and evolutionary strategies for multiobjective pareto-optimization in electromagnetics. Int J Appl Electromagn Mech 2001;15:231–6.
[81] Wilson B, Cappelleri D, Simpson TW, Frecker M. Efficient Pareto frontier exploration using surrogate approximations. Optim Eng 2001;2:31–50. https://doi.org/10.1023/A:1011818803494.
[82] Ruzika S, Wiecek MM. Approximation methods in multiobjective programming. J Optim Theory Appl 2005;126:473–501. https://doi.org/10.1007/s10957-005-5494-4.
[83] Martín J, Bielza C, Insua DR. Approximating nondominated sets in continuous multiobjective optimization problems. Nav Res Logist NRL 2005;52:469–80. https://doi.org/10.1002/nav.20090.
[84] US EPA O. Technical update of the social cost of carbon for regulatory impact analysis under executive order 12866 (May 2013, Revised August 2016) [WWW Document]; 2016. <https://www.epa.gov/climatechange/social-cost-carbon> [accessed 3.8.17].
[85] Moore FC, Diaz DB. Temperature impacts on economic growth warrant stringent mitigation policy. Nat Clim Change 2015;5:127–31. https://doi.org/10.1038/nclimate2481.
[86] Rusu M. Social cost of carbon: opportunities and environmental solutions. Procedia econ. finance, international conference emerging markets queries in finance and business, Petru Maior University of Tîrgu-Mures, Romania, October 24th–27th, 2012 2012. p. 690–7. https://doi.org/10.1016/S2212-5671(12)00215-8.
[87] Nordhaus WD. Revisiting the social cost of carbon. Proc Natl Acad Sci. 2017;114:1518–23. https://doi.org/10.1073/pnas.1609244114.
[88] Van Grinsven HJM, Holland M, Jacobsen BH, Klimont Z, Sutton MA, Jaap Willems W. Costs and benefits of nitrogen for Europe and implications for mitigation. Environ Sci Technol 2013;47:3571–9. https://doi.org/10.1021/es303804g.
[89] Keeler BL, Gourevitch JD, Polasky S, Isbell F, Tessum CW, Hill JD, et al. The social costs of nitrogen. Sci Adv 2016;2:e1600219. https://doi.org/10.1126/sciadv.1600219.
[90] Compton JE, Harrison JA, Dennis RL, Greaver TL, Hill BH, Jordan SJ, et al. Ecosystem services altered by human changes in the nitrogen cycle: a new perspective for US decision making. Ecol Lett 2011;14:804–15. https://doi.org/10.1111/j.1461-0248.2011.01631.x.
[91] Wu X, Zheng Y, Wu B, Tian Y, Han F, Zheng C. Optimizing conjunctive use of surface water and groundwater for irrigation to address human-nature water conflicts: a surrogate modeling approach. Agric Water Manage 2016;163:380–92. https://doi.org/10.1016/j.agwat.2015.08.022.
[92] Kim IY, de Weck OL. Adaptive weighted sum method for multiobjective optimization: a new method for Pareto front generation. Struct Multidiscip Optim 2006;31:105–16. https://doi.org/10.1007/s00158-005-0557-6.
[93] Hartikainen M, Miettinen K, Wiecek MM. PAINT: Pareto front interpolation for nonlinear multiobjective optimization. Comput Optim Appl 2012;52:845–67. https://doi.org/10.1007/s10589-011-9441-z.
[94] Lotov A, Bushenkov VA, Kamenev GK. Interactive decision maps: approximation and visualization of Pareto frontier. Springer Science & Business Media; 2013.
[95] NRCS-USDA. Soil survey staff, natural resources conservation service, United States Department of Agriculture. Soil Survey Geographic (SSURGO) database [WWW Document]; 2014. <https://sdmdataaccess.sc.egov.usda.gov> [accessed 6.20.14].
[96] Pervez MS, Brown JF. Mapping irrigated lands at 250-m scale by merging MODIS data and national agricultural statistics. Remote Sens 2010;2:2388–412. https://doi.org/10.3390/rs2102388.
[97] NASS-CDL. CropScape – national agricultural statistics services – crop data layer program [WWW Document]; 2016. <https://nassgeodata.gmu.edu/CropScape/> [accessed 8.1.16].